Far-infrared studies of the cyclotron-resonance line shape of two-dimensional electrons in silicon in the quantum limit

J.-P. Cheng and B. D. McCombe
Department of Physics and Astronomy, State University of New York at Buffalo, Buffalo, New York 14260
(Received 11 March 1991)

Systematic far-infrared magneto-optical measurements of cyclotron-resonance spectra of quasi-two-dimensional electrons have been carried out on a series of *n*-channel Si metal-oxide-semiconductor devices with a wide range of mobilities (4500 to $>10\,000$ cm^2/V s) at very low electron densities (1.0×10^{10} to 8.8×10^{11} cm^{-2}), low temperatures (2–40 K), and high magnetic fields (up to 15 T). A *multiple-line structure* with at least three distinct components in a crossover region of intermediate Landau-level filling factors (the Landau-level occupancy) has been observed. The "anomalous" behavior in the line shapes and an observed apparent upward shift in resonance frequency at the lowest filling factors result from the relative intensity variation of individual components as a function of filling factor. The observed *systematic* correlation of the magnitude of the anomalies with the inverse of the sample mobility demonstrates the importance of localization. The effects of magnetic field, temperature, substrate bias, and surface band structure on these characteristics have been investigated. Results are compared with theoretical models and recent experimental work on an alternative system (GaAs heterostructures). It is argued that both localization and electron-electron correlations play important roles and must be considered on an equal footing in explaining the anomalous behavior in the low-density regime.

I. INTRODUCTION

Reduced-dimensionality electronic systems have attracted considerable attention for the last 10–20 years in semiconductor physics. Various quasi-two-dimensional (2D) structures, in which the carrier motion is confined in one direction and free in other directions, have been practically realized and extensively studied.[1] These studies have led to several very important discoveries in basic physics (e.g., the integer and fractional quantum Hall effects[2,3]) and the creation of structures that have electronic or optoelectronic applications (high-mobility transistors and quantum-well lasers). Quasi-2D systems such as Si metal-oxide-semiconductor (MOS) structures and modulation-doped GaAs/$Al_xGa_{1-x}As$ heterostructures provide a nearly ideal physical testing ground for exploring our understanding of many interesting phenomena, such as many-body effects, interface scattering, 2D localization, and so on. These effects are very important in the electronic and optical properties of 2D systems and are generally enhanced by the confinement in one direction. The Si-MOS device is particularly well suited for such investigations because the carrier concentration in the inversion layer can be varied independently and determined with reasonable precision over a wide range. The net density of charged interface impurities and the carrier wave-function extent from the interface can also be readily determined.

In the presence of a uniform magnetic field along the confinement direction, the electron motion is completely quantized into Landau levels. Cyclotron resonance (CR) is a fundamental measurement of transitions between these fully quantized states, and it provides a powerful tool to study the dynamical properties of the 2D electron gas. Under the usual experimental conditions, the resonance position and line shape are related to the effective mass and scattering time in a simple way. In principle, the quantum limit condition, when all electrons are in the lowest Landau level, provides the simplest situation for line-shape analysis. However, at extremely low densities and high magnetic fields the resonance shows numerous anomalies which have been reported for various 2D systems. Extensive experimental investigations have been carried out with results interpreted by widely varying theoretical models.[4] Previous work on inversion layers in Si-MOS devices[5–7] led to several theoretical interpretations: single-particle localization by random-potential fluctuations,[8] the possibility of a Wigner lattice,[6] and pinned charge-density waves,[9] or a Wigner glass.[7] Recent work on GaAs/$Al_xGa_{1-x}As$ heterostructures has revealed additional features[10–16] and produced additional theoretical models: interaction with magnetoplasmons,[10] magnetic excitons,[17] and influence of the fractional quantum Hall effect.[15,16] At present, none of these theoretical models is well established, and there is not yet a clear physical picture that unifies all of the anomalies observed in various low-density CR experiments.

We have carried out a systematic experimental investigation of cyclotron resonance on a series of Si-MOS samples with a wide range of peak effective mobilities at low temperatures, low electron densities, and in magnetic fields up to 15 T.[18] The sample properties were characterized by dc transport and magnetotransport measurements at liquid-He temperatures. Extensive far-infrared (FIR) magneto-optical measurements were made with a Fourier-transform spectrometer in conjunction with 9- and 15-T superconducting magnets. Various samples and external parameters, such as filling factor, magnetic field,

temperature, substrate bias, electron density, and orientation of the crystallographic plane, were investigated systematically. The magnetotransmission measurements exhibit a single CR line at high densities, a clear *multiple-line structure* in a crossover region of intermediate densities, and a sharp line at very low densities that is shifted to higher frequencies by an amount that correlates inversely with the sample mobility. The observation of a multiple-line structure, unrelated to population of higher valleys in the Si conduction band, and the systematic correlation of the magnitude of the anomalies with the inverse of the sample mobility provide a new perspective on this problem and demonstrate the importance of localization *as well as* many-body effects. Experimental details, including sample description and characterization via transport techniques, are presented in Sec. II. In Sec. III, results of FIR optical measurements under various experimental conditions are provided. Detailed comparisons between the present CR experimental results and the existing theoretical models are made in Sec. IV. A summary and overall conclusions of this work are offered in Sec. V.

II. EXPERIMENTAL DETAILS

A. Samples and sample characterization

All Si-MOS devices investigated in this work have large gate area (2.5×2.5 mm^2) and are fabricated on p-type Si substrates that are nominally doped with boron impurities at $3\times10^{14}-1\times10^{15}$/cm^3 (resistivities were about 10–30 Ω cm). The surface orientations were vicinal to the [001] direction with the largest tilt angle equal to $\sim10°$ (sample 3). The oxide thicknesses are all near 2000 Å, and standard optical lithographic and phosphorous diffusion processes were used to develop the source and drain Ohmic contacts. Samples 1, 2, and 3 have semitransparent chromium gates fabricated as part of the processing for FIR transmission experiments. Sample 4 was originally fabricated with a thick aluminum gate, which was removed by standard metal etch processing, and a thin semitransparent chromium gate was then reevaporated in vacuum. After these processes this sample showed an interesting electric field stress effect; i.e., the low-temperature transport properties were affected by the history of the applied gate voltage during the sample cooling process; a negative gate voltage stress reduced the mobility, and a positive one increased the mobility with peak mobility ranging from 10 000 to 12 500 cm^2/V s. This effect can be explained by mobile negative charges injected into the SiO_2 dielectric layer, probably into the interfacial region between the original insulator and a new, thin oxide created after etching or during the remetallization procedure.

To avoid Fabry-Pérot interference the substrates of the samples were wedged by grinding at angles of about 5°–10°. The substrate-wedged sample then was glued on a brass sample holder with a piece of black polyethylene filter mounted underneath the sample. In this configuration, the sample front surface is directly exposed to broadband radiation from the spectrometer and room-temperature radiation, so that the inversion layer is optically pumped very weakly; this enhances the charging and discharging rate of the inversion and depletion regions with gate modulation at low temperatures.

Characterization of sample properties was accomplished via transport and magnetotransport techniques, primarily dc conductance and transconductance measurements. With the usual capacitor model the relationship between the 2D electron density in the inversion layer n_s and the gate voltage V_G can be written as[19]

$$n_s=(\epsilon_{ox}/d_{ox}e)(V_G-V_{th})\equiv\alpha(V_G-V_{th}) , \quad V_G>V_{th} , \tag{1}$$

where ϵ_{ox} and d_{ox} are the static dielectric constant and the thickness of the SiO_2 layer, respectively. The parameter, $\alpha\equiv\epsilon_{ox}/d_{ox}e$, and the threshold voltage V_{th} were determined experimentally from Shubnikov–de Haas (SdH) oscillations at 4.2 K, and fan diagrams.[1] The threshold voltage is sensitively dependent on the depletion charge,[19] which can change slightly from time to time due to nonequilibrium buildup during the cooling process. In order to have an accurate n_s-V_G relation, SdH measurements had to be performed each time the sample was cooled down to account for possible variations in depletion charge.

Another important macroscopic parameter to describe the properties of electron motion in the inversion layer is the low-temperature effective mobility μ_{eff}, which is directly related to the dc sheet conductivity σ_s by

$$\mu_{eff}=\sigma_s(V_G)/n_s(V_G)e . \tag{2}$$

The sheet conductivity can be determined from the experimentally measured channel conductance at particular values of V_G, and the sheet electron density can be independently measured as discussed above. In general, the effective mobility is a function of gate voltage; the *peak* value is normally used as the parameter to describe the sample quality. The activation energy and the number density of localized states have also been measured via the temperature-dependent conductance studies.[1] Samples with higher peak effective mobility have smaller activation energies and fewer localized states per unit area; the latter is roughly $(1.5–4.0)\times10^{11}$ cm^{-2} between the highest- and the lowest-mobility samples used in this work. The important parameters for the samples are summarized in Table I.

TABLE I. Summary of sample characteristics measured via dc transport and magnetotransport techniques. Measurements were made at 4.2 K.

Sample no.	Surface orientation	Peak mobility (cm^2/V s)	Electron density (cm^{-2} V^{-1})
1	(001)	4 500	1.2×10^{11}
2	(001)	5 600	1.3×10^{11}
3	(118)	7 000	8.2×10^{10}
4	$\sim1°$ tilt	10 000	8.5×10^{10}

B. FIR optical measurements

A block diagram of the experimental setup is shown in Fig. 1. A commercial slow-scan Fourier transform spectrometer (including the interferometer, the light source, and the mirror drive) was used in a repetitively scanned mode in conjunction with a 9-T (at Buffalo, NY) or a 15-T [at the Francis Bitter National Magnet Laboratory (FBNML), Cambridge, MA] superconducting magnet. The scan control of the stepper motor which drives the movable mirror in the spectrometer and the Fourier analysis of the data after the signal averaging over multiple scans were all performed by a microcomputer system with appropriate interfacing and software. The FIR output of the spectrometer is directed by a brass light pipe and an adjustable Al-coated (or polished brass) mirror to the polyethylene window of the stainless-steel-light-pipe–sample-holder system, which is sealed in a thin-walled stainless-steel tube (vacuum jacket), and placed inside a superconducting magnet Dewar. The light is focused on the sample by a condensing cone, and the light transmitted through the sample is further guided by light pipe and light cone optics through a wedged sapphire window into a vacuum can and then into the bolometer detector housing, which is maintained at a temperature near 1.6–1.7 K by thermal contact with a cold plate in contact with a continuous flow refrigerator.[20] A commercial Si-composite bolometer detector converts the light signal into an electrical voltage output which is fed into a lock-in amplifier. The reference frequency of the amplifier is determined either by the chopper frequency, which modulates the light output of the spectrometer, or by the frequency of the gate-modulation voltage applied to the sample. The dc voltage output of the amplifier is then digitized and stored in the computer for each mirror position. The resultant interferogram is obtained after the completion of one mirror scan (or multiple scans when signal averaging is required). Fourier transformation then is performed by computer to convert the interferogram into a spectrum. All data shown in this paper have the same resolution, about 3 cm^{-1}.

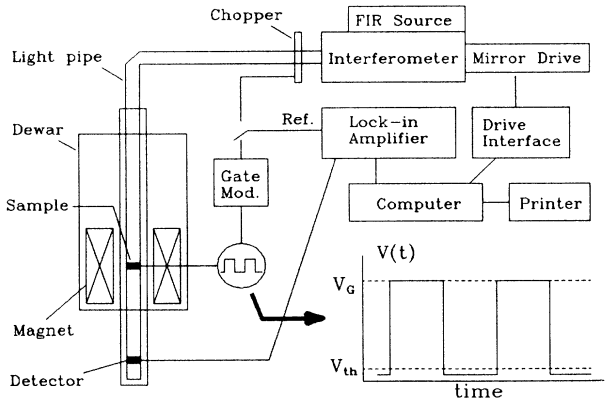

FIG. 1. Block diagram of experimental setup. The inset shows the square wave gate modulation and its relation to V_G and V_{th}.

A differential gate-modulation technique was used in this experiment to enhance the signal-to-noise ratio (see the inset of Fig. 1). The square wave from a wave generator is set with the "lower" voltage slightly below the threshold voltage of the device (corresponding to $n_s=0$) and the "upper" voltage equal to some desired value above threshold which corresponds to a certain electron density through the n_s-V_G relation [Eq. (1)]. Low modulation frequencies (20–100 Hz) were used due to the bolometer's low-frequency response and the charging time of the MOS device at low temperatures and small gate voltages (in the region of localization). The chopper in the spectrometer was stopped at an "open" position, so that the sample surface was continuously illuminated with light. The normalized spectrum was obtained by ratioing the differential spectrum $[T(n_s)-T(n_s=0)]$ to a background obtained by chopping the FIR light source.

III. RESULTS AND ANALYSES

A. Filling factor dependence

Figures 2(a)–2(d) are normalized differential absorption spectra for four samples at 9 T and 4.2 K. We first concentrate on Fig. 2(a) which shows results for the lowest-mobility sample (sample 1). At high electron densities, or equivalently large Landau-level filling factor ν ($\nu=hcn_s/eB$), when the magnetic field B is fixed, CR is a single, symmetric, and reasonably sharp line with linewidth approximately satisfying the relation of inverse proportion to the sample mobility. The resonance shifts slightly to lower frequency as ν is reduced. When the filling factor is reduced below some critical value ν_c, which is about 3 for this sample, a dramatic change in the line shape occurs; a new feature appears on the high-frequency side (initially as a shoulder) which causes the line shape to be strongly asymmetric when it is not well resolved. As ν is reduced further, a multiple-line structure can be clearly observed [indicated as 1, 2, and 3 in addition to the original CR peak in Fig. 2(a)], and the overall "linewidth" becomes *extremely* large. The relative intensities of the lower-frequency components decrease rapidly as ν is reduced; thus the overall "linewidth" dramatically narrows, and the center of gravity (defined operationally as the frequency for which the integrated intensity above is equal to that below this frequency) moves quickly to the position of the high-frequency line. In the lowest filling factor region ($\nu<1.3$ for this sample), the highest-frequency peak (line 3) becomes the dominant line with the linewidth significantly narrower than that of the high-density CR line. It shifts slightly to lower frequency as ν is reduced further.

The evolution of the line positions for the multiple-line structure with filling factor ν is shown in Fig. 3 for sample 1. Lines 1 and 2 are observable only in a narrow filling factor range ($1.3<\nu<2.5$) with line 1 shifting down and line 2 shifting up as ν decreases. Line 3 is first observable as a high-frequency shoulder near $\nu=3$, and it increases in relative intensity with no dramatic frequency shift all the way down to the lowest filling factors.

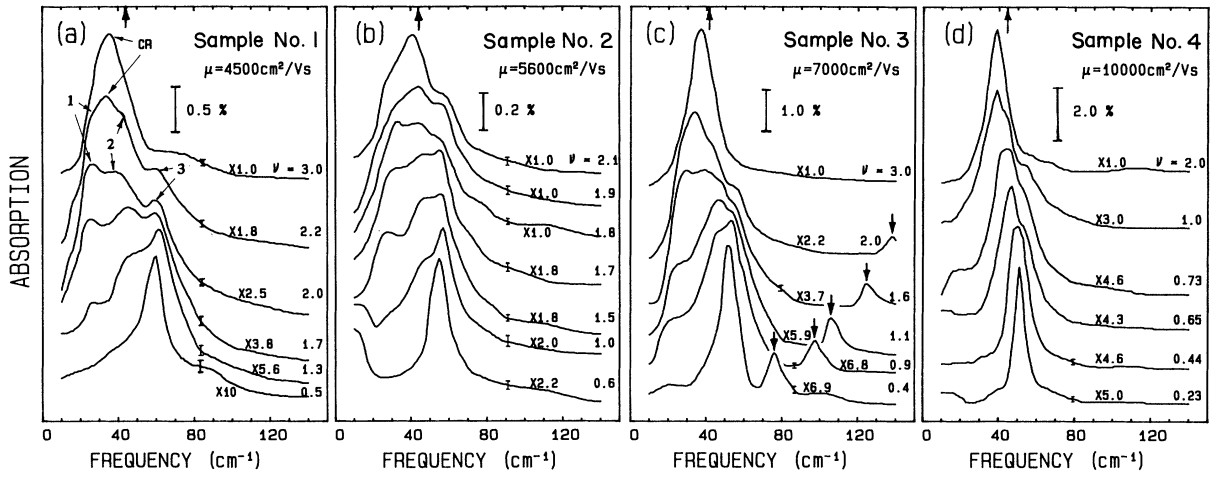

FIG. 2. Filling factor dependence of CR line shape for four samples with different mobilities at 9 T and 4.2 K. The arrow at the top of each panel shows the position of unperturbed CR defined by the bulk effective mass for the twofold valleys. Features indicated by downward arrows in (c) are intersubband transitions due to surface tilt. Bars indicate the noise level.

B. Sample mobility dependence

Similar measurements have been carried out on several other samples with different mobilities. The results for four samples at the same magnetic field, 9 T, and temperature, 4.2 K, are plotted in Fig. 2, side by side in order of increasing mobility. Comparing the four panels we see that the general features of CR line shape for different samples are quite similar. The high-frequency features indicated by the downward arrows in panel (c) are intersubband transitions due to the anisotropic band structure of silicon;[21] otherwise varying the surface crystallographic plane has no discernible effect. At large filling factors, the CR linewidth is qualitatively related to sample mobility by the usual inverse proportionality. In the intermediate ν region, the lower-mobility samples have larger values of ν_c, which varies roughly from 3 to 1 between the lowest- and the highest-mobility samples, and clearer multiple-line structure. For the highest-mobility sample only CR and line 3 are clearly observed, with line 3 first appearing as a shoulder at $\nu \simeq 1$ and becoming the dominant, sharp feature below $\nu \simeq 0.4$. There is some indication of line 2 between $\nu = 1$ and 0.4 in Fig. 2(d), but it is not clearly resolved. There is no clear indication of line 1 in this sample. In the lowest ν region ($\nu < 0.4-1.3$ between the highest- and lowest-mobility samples), the linewidth exhibits only a weak sample dependence (full width at half maximum, FWHM, is $\sim 8-10$ cm^{-1} between the highest- and lowest-mobility samples). The simple relationship between linewidth and scattering time is clearly not valid in this low filling factor region.

In Fig. 4 the center of gravity of the multiple-line structure is plotted as a function of filling factor ν for all samples at 9 T with respect to the unperturbed CR position [defined by the bulk cyclotron mass, $0.191m_0$ for the (001) surface and $0.204m_0$ for the (118) surface with m_0

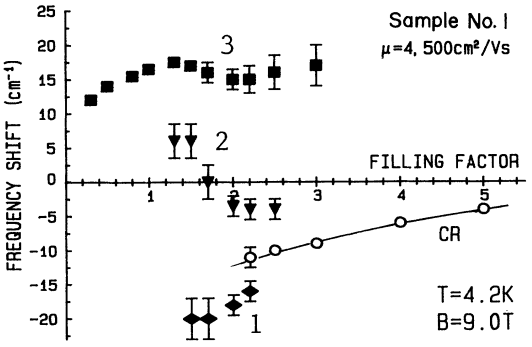

FIG. 3. Evolution of the multiple-line structure for sample 1. The shifts of the peak positions relative to the unperturbed CR are plotted as a function of filling factor. The different symbols are used to indicate the different (numbered) features and cyclotron resonance (CR).

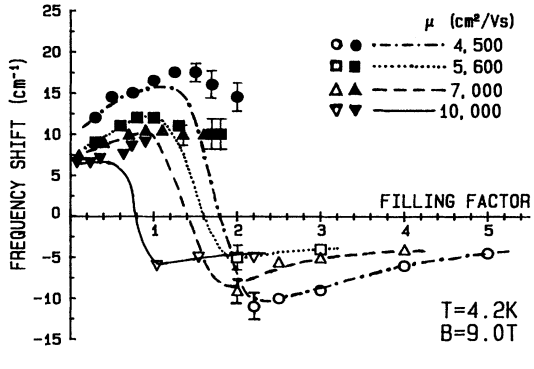

FIG. 4. Peak position shift from the unperturbed CR. Curves are the center of gravity (as defined in the text) of the complex line for four samples. Open symbols: CR positions at high ν; solid symbols: positions of the sharp line at the lowest values of ν.

the free-electron mass]. At the highest and the lowest values of ν, the center of gravity is the position of CR (open symbols) and line 3 (solid symbols), respectively, since only a single line appears in these regions. At intermediate values of ν, the center of gravity is the frequency most likely to be chosen as the "CR" position when the multiple-line structure is not well resolved; thus it can be used to compare with the early work (e.g., Ref. 7). The frequency shift of the sharp absorption peak at the lowest densities from the unperturbed CR position increases systematically from about 7 to 15 cm^{-1} between the highest- and lowest-mobility samples. The graph also illustrated the systematic mobility dependence of the critical filling factor ν_c alluded to above, i.e., a continual reduction in ν_c as mobility increases. Regarding the center of gravity as a function of ν, the results shown here are very similar to the earlier work on Si.[7] However, the ν dependence is not universal as suggested in the earlier work. The detailed line shape and the critical filling factor ν_c depend on sample mobility in a systematic way.

C. Magnetic-field dependence

It is important to identify whether the filling factor ν or the electron density n_s is the major parameter involved in determining the CR line shape since different theoretical models are distinguishable on this basis. The judgment can be experimentally made by examining measurements carried out over a wide range of magnetic field.

In Fig. 5 we show CR spectra on sample 3 at several magnetic fields with fixed 2D electron density at $n_s = 1.93 \times 10^{11}$ cm^{-2}. This value was chosen so that the corresponding filling factors cover the region where the line shape exhibits dramatic changes as magnetic field is varied. The filling factor values are displayed in the brackets following the corresponding magnetic fields for each curve in this figure for convenience in comparing with Fig. 2(c). The upward arrows indicate the unperturbed CR position, and the downward ones indicate the intersubband transition due to the tilted surface, which does not move with magnetic field when n_s is fixed. At the lowest magnetic field (4 T and $\nu = 2.2$), the dominant transition is located at CR frequency, and the multiple-line structure can be barely distinguished. As magnetic field is increased (ν reduced), the high-frequency components of the multiple-line structure constantly increase in relative intensity. The highest-frequency component becomes the dominant peak at the highest field (9 T and $\nu = 0.9$). The line shape changes dramatically, and the center of gravity moves continuously to higher frequency with respect to the unperturbed CR position as the field increases (ν decreases). This demonstrates that the electron density n_s is not the major parameter correlated with CR line shape. On the other hand, if we compare the spectra with Fig. 2(c), they are quite similar for the same values of ν within the noise level, which demonstrates the crucial role of the filling factor.

The filling factor dependence of the CR line shape shown in Fig. 2 has also been studied at several magnetic fields other than 9 T. An example of such studies on sample 3 is shown in Fig. 6 [6(a) and 6(b)]. In Fig. 6(a) we show the data taken at 6 T and 4.2 K with the filling factors covering the same region as in Fig. 2(c). Detailed comparison between Figs. 6(a) and 2(c) leads to the conclusion that the filling factor is the major parameter in determining the line shape within this magnetic-field region and the experimental error involved in the electron density measurements, different background, signal-to-

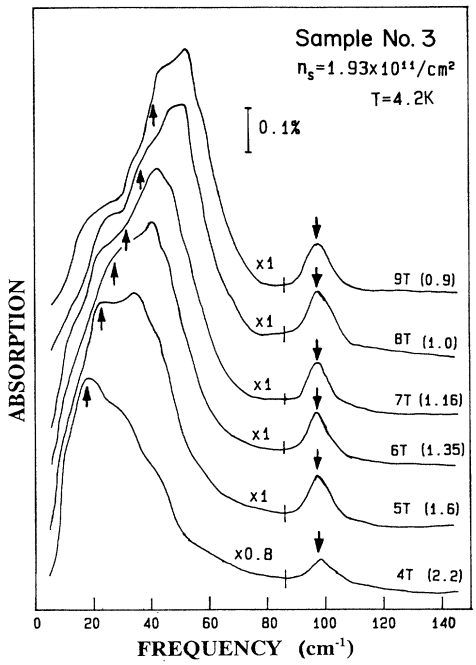

FIG. 5. Differential absorption spectra at fixed electron density and various magnetic fields. Numbers in parentheses are the corresponding filling factors. The upward arrows indicate the unperturbed CR positions, and downward ones indicate the intersubband transitions.

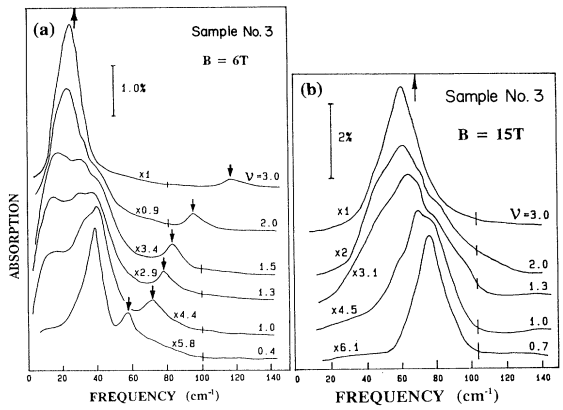

FIG. 6. Filling factor dependence of the line shape for sample 3 at fixed magnetic fields of (a) 6 T and (b) 15 T, at a temperature of 4.2 K. The unperturbed CR position is indicated by upward arrow at each field. The intersubband transitions are indicated by downward arrows in (a) and are at much higher frequency (out of scale) in (b).

noise ratio, etc. To exclude the uncertainty due to the limited range of magneticfields available at Buffalo, we extended the studies with a 15-T superconducting magnet at FBNML with the results shown in Fig. 6(b). The qualitative behavior of CR is the same as in Fig. 2(c) or Fig. 6(a). The linewidth in this measurement is larger than that in the low field measurements. For large filling factors, this linewidth broadening is probably due to short-range scattering,[1] i.e., linewidth $\propto B^{1/2}$, and substantially larger surface scattering at larger gate voltages. In the lowest ν region (the lowest filling factor data at this magnetic field are at $\nu=0.7$), the broadening might be due to larger fluctuation potentials relative to the electron-electron interaction at larger surface electric field, which is qualitatively consistent with the results of mobility-dependent and substrate-bias-dependent measurements (see below), and the prediction of the single-particle localization model as discussed in the final part of this paper. Although the signal-to-noise ratio is not as good as that in the low field measurements, this result confirms that the filling factor is indeed the major parameter that correlates with the line shape for a given sample.

We summarize the magnetic-field-dependent studies on this sample, represented in Figs. 2(c), 6(a), and 6(b), by plotting the peak position shift (CR at high densities and line 3 at the lowest densities) from the unperturbed CR position as a function of ν at three magnetic fields in Fig. 7. Notice that special care is needed in determining the position of line 3 when the intersubband transitions are close to it at low densities since the interaction between the two transitions will cause a repulsion from each other.[21] The broken line is the center of gravity at 9 T. It is clear that the qualitative behavior is the same over this region of magnetic fields; the critical filling factor ν_c and the shift of position (line 3) relative to the unperturbed CR in the lowest ν region exhibit no noticeable changes within experimental error. Similar studies were also carried out on other samples with results consistent with the conclusions reached for sample 3.

The magnetic-field effects on the sharp line in the lowest filling factor region have been studied in detail. Results on sample 4 are shown in Fig. 8 for a fixed filling factor, $\nu\simeq 0.3$, and temperature, 4.2 K. The line shape exhibits no dramatic change as the field varies from 4 to 9 T (electron density changes more than a factor of 2 at constant ν). The linewidths and the shifts upward in position from the unperturbed CR are independent of magnetic field in this field region within experimental error.

D. Temperature dependence

Measurements of the temperature dependence were carried out between 2.2 and 40 K at various filling factors. Temperature elevation (above 4.2 K) was accomplished by passing dc currents (<50 mA) through a ~ 100-Ω resistive heater wound noninductively on a brass heater housing in thermal contact with the sample holder. Temperatures were measured with a calibrated capacitance sensor mounted in the brass housing. Temperatures lower than 4.2 K were achieved by pumping on the sample chamber of the magnet Dewar to reduce the vapor pressure of liquid helium, and temperatures were determined from standard temperature–He-vapor-pressure calibration tables with the vapor pressures measured by a commercial Baratron gauge.

Figure 9(a) shows the absorption spectra taken on sample 4 for several temperatures at a fixed magnetic field, 9 T, and filling factor $\nu=1.0$ (chosen to be around ν_c for this sample). At low temperature, the multiple-line structure can be clearly seen with the high-frequency components appearing as shoulders. As temperature is raised, these shoulders continuously increase in relative intensity and broaden (the highest-frequency line is hard

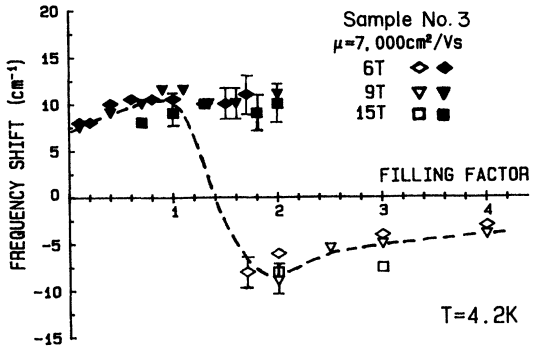

FIG. 7. Peak position shift from the unperturbed CR for sample 3 at three magnetic fields. Open (solid) symbols are transitions at high (low) filling factors. The dashed line is the center of gravity of the complex lines at 9 T.

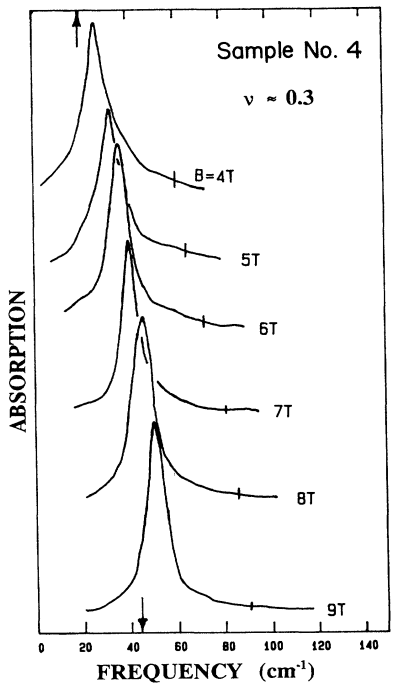

FIG. 8. Magnetic-field dependence of the absorption spectra at a fixed value of ν in the lowest ν region for sample 4. The upward (downward) arrow at the top (bottom) indicates the unperturbed CR position at 4 T (9 T).

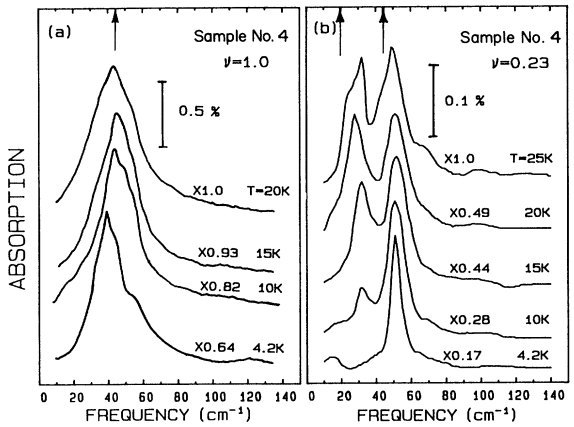

FIG. 9. Temperature dependence of the absorption spectra for sample 4 at a magnetic field of 9 T in different filling factor regions. (a) $\nu=1.0$; arrow at the top is the position of unperturbed CR. (b) $\nu=0.23$; the two arrows at the top indicate the unperturbed CR for twofold valleys ($m^*=0.191m_0$, higher frequency) and fourfold valleys ($m^*0.481m_0$, lower frequency).

to resolve at slightly elevated temperatures), and the center of gravity shifts slightly to higher frequency. For $T\geq 15$ K, the multiple-line structure is completely smeared out, and CR is a broadened, symmetric line with peak position located at approximately the average position of the multiple-line structure, which is quite close to the unperturbed CR position (indicated by the upward-pointing arrow at the top of the graph).

At the lowest filling factors, the temperature effect on the line shape for this sample is dramatic, as shown in Fig. 9(b). As temperature increases, the sharp line, which is shifted to high frequency from the unperturbed CR, broadens and loses intensity, while a new transition appears at lower frequency with relative intensity increasing. At high temperatures ($T\geq 20$ K), a distinct double-line structure can be observed. Similar measurements have been performed at other electron densities (or ν when the field is fixed) and on other samples. The double-line structure is more distinct and appears at lower temperature when the electron density (therefore the electric field) is smaller.

The lower-frequency line is attributed to cyclotron resonance of localized electrons in higher-lying fourfold degenerate valleys. It has been shown that the localized states in a band tail can extend well below the mobility edge,[22] an estimate shows that the subbands associated with the fourfold degenerate valleys can be thermally occupied at fairly low temperature when electron and depletion charge densities are very small. The fact that temperature effects on the line shape are more distinct at lower n_s is due to the weaker interface electric field and the concomitant smaller splitting between twofold and fourfold valleys. Substrate-bias-dependent studies of this double-line structure (discussed in the last part of this section) show that the intensity of the lower-frequency peak depends sensitively on substrate bias voltage at the same temperature and the same n_s, which further confirms the hypothesis. The magnetic-field-dependent measurements also give consistent results. The arrows at the top of the graph indicate the unperturbed CR positions for twofold valleys (higher frequency) and fourfold valleys (lower frequency). The transition of fourfold valleys is also shifted upward by about 10 cm^{-1} from the unperturbed CR. This is slightly larger than the shift observed for the twofold valleys and is consistent with the single-particle localization model as discussed below. For the sharp line associated with twofold valleys, increasing temperature broadens the linewidth slightly; however, it hardly changes the peak position. *No* distinguishable transition is observed at the unperturbed CR position even at the highest temperature in the measurements (35 K, not shown in the figure), contrasting with the results of $\nu=1.0$ in Fig. 9(a).

E. Substrate bias dependence

The depletion charge density (2D) and surface electric field can be conveniently changed by applying a substrate-to-source voltage, V_{SB}.[19] With a negative V_{SB}, the depletion charge density and the surface electric field increase. At a fixed n_s, the subband separation becomes larger, and the threshold voltage shifts to a higher value, necessitating an increase in V_G to keep n_s constant. The n_s-V_G relation thus has to be redetermined for each substrate bias value in order to obtain accurate values of n_s from V_G in the gate-modulation technique.

The substrate-bias-dependent studies of CR were carried out on sample 4, the only sample with a reliable substrate contact (sintered Al top-side contact) in this work. Figure 10 shows the spectra at a fixed magnetic field of 9

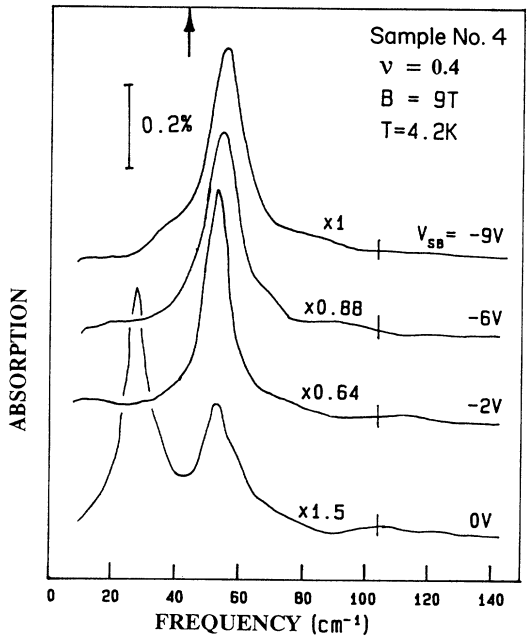

FIG. 10. Substrate bias dependence of absorption spectral for sample 4 at $\nu=0.4$, $B=9$ T, and $T=4.2$ K. The lower-frequency peak in the spectrum for $V_{SB}=0$ is due to the transition of localized electrons in the band tail of fourfold valleys.

T, a temperature of 4.2 K and $\nu=0.4$. In this experimental run, CR of localized electrons for the fourfold valleys can be observed with quite strong intensity relative to that for twofold valleys at this density and temperature; indicating an extremely weak effective surface field at zero substrate bias voltage. When $V_{SD}=-2$ V, the transition for fourfold valleys completely disappears and a single sharp line is observed. This is easily understood since the reverse substrate bias with the accompanying increase in surface electric field increases the subband separation. When V_{SD} is varied from -2 to -9 V, the peak position shifts upward about 3 cm^{-1} and the linewidth (FWHM) broadens from 10 to 14 cm^{-1}.

IV. COMPARISON WITH THEORETICAL MODELS

There are a number of theoretical models that have been proposed to explain the various anomalies in low-density cyclotron-resonance spectra. These models can be generally categorized into two types: (1) single-particle localization models which consider electrons trapped in individual potential wells resulting from the random fluctuations of interface potential; and (2) modes that make recourse to many-body effects due to the Coulomb interaction among the electrons. In this section, we compare our experimental results with several models that are most closely related with this problem.

A. Single-particle localization

In this very simplified model, the random-potential fluctuations at the interface are treated as a limited set of simple harmonic oscillators with different characteristic frequencies ω_0.[7,8] For electrons trapped in such oscillator potentials the allowed electric dipole transitions in the presence of a uniform external magnetic field normal to the interface occur at frequencies

$$\omega_{\pm}=\tfrac{1}{2}[(\omega_c^2+4\omega_0^2)^{1/2}\pm\omega_c]\ , \tag{3}$$

where ω_+ represents the upward-shifted cyclotron frequency with the electron motion coupling to the CR-active circularly polarized light, and ω_- is the frequency of anticyclotron motion of the orbit center coupling to the CR-inactive light due to the scattering from the potential walls. The linewidth of the transitions depends on the inhomogeneous broadening due to different ω_0's.

Despite its simplicity this model can explain qualitatively the upward transition-frequency shift of localized electrons with a systematic mobility dependence (the poorer mobility samples have stronger localization; effectively larger ω_0), the larger frequency shift for the fourfold valley than twofold valleys (smaller ω_c), and the substrate-bias-dependent results (reverse substrate bias increases the surface field, and thus increases ω_0). However, several important experimental facts cannot be explained by this model. (i) The sharpness of the line at the lowest values of ν. The line should be inhomogeneously broadened by the distribution of random potentials (harmonic-oscillator potentials in this model). (ii) The ν-dependent behavior for a given sample. The model predicts that the electron density (more accurately the density of localized states), not the filling factor, is the critical parameter determining the line shape. (iii) The multiple-(3–4) line structure near ν_c. This model yields, at most, two lines in addition to CR, and the lower branch occurs at too low a frequency at the fields used in the experiments to be detected; it is significantly lower than line 1 discussed previously. A comparison between Eq. (3) and experimental results is shown in Fig. 11, where ω_0 is used as a parameter to fit (solid lines) the data (solid dots) taken at fixed filling factor $\nu\approx0.3$ on sample 4 (the spectra are shown in Fig. 8). Within the experimental error the ω_+ branch can fit the data reasonably well in the lowest filling factor region. On the other hand, the peak positions can also be fit equally well with a straight line (dotted line) parallel to the unperturbed CR (broken line) as suggested in Ref. 7. More sophisticated model calculations have been performed based on the same single-particle localization picture.[7,8] They suffer the same general shortcomings as discussed above.

B. Pinned charge-density wave

Electron correlations play a very important role in the low-density cyclotron resonance since the Coulomb energy is one of the most important energies in this problem ($\sim$4–5 meV at $n_s\sim5\times10^{10}$ cm^{-2}). In a strong magnetic field the only degree of freedom for 2D electrons is the motion of the CR orbit center. At sufficiently low temperature (below 1 K), the repulsive Coulomb interaction will keep such classical particles apart to minimize the total energy, and electrons can be crystallized.[23] The temperatures used for most of the CR experiments are

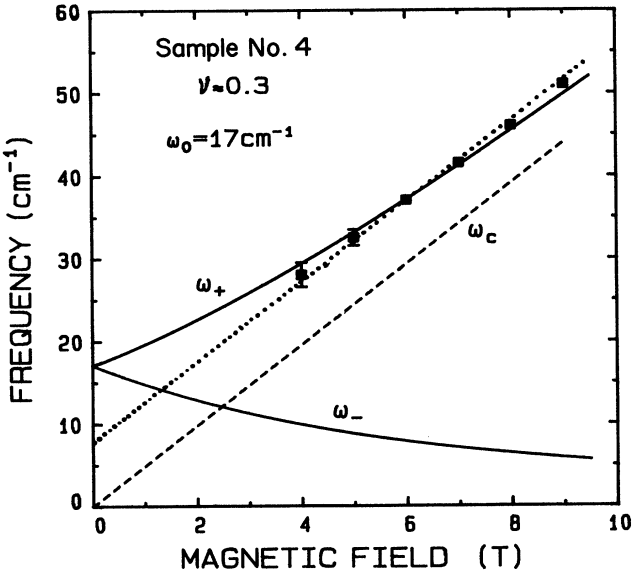

FIG. 11. Magnetic-field dependence of transition frequencies. Experimental data (solid squares) are compared with the single-particle localization calculation, ω_+ and ω_- (solid lines). The dashed line is the unperturbed CR, and the dotted line is a linear fit parallel to CR.

around 4.2 K, and we can only expect short-range order.

The charge-density wave is a related type of order due to electron-electron correlation. Fukuyama and Lee[9] have developed a model of two-dimensional charge-density waves in a magnetic field pinned by short-range impurity centers having identical potential amplitude, but distributed randomly in space. In the long-wavelength limit, two resonant transitions are predicted with frequencies given by

$$\Omega_{\pm}^2=\tfrac{1}{2}[\omega_c^2+2\gamma^2\pm\omega_c^2(1+4\gamma^2/\omega_c^2)^{1/2}]\ , \tag{4}$$

where γ is the pinning parameter proportional to the amplitude of the spatial variation of charge density, the number density of impurity centers, and the square of the amplitude of impurity potentials. The oscillator strengths are determined from

$$A_{\pm}=(n_s e^2\pi/2m^*)[1\pm(1+4\gamma^2/\omega_c^2)^{1/2}]\ , \tag{5}$$

and the linewidths are the same for both modes: $\Gamma\sim\alpha\gamma^2/\omega_c$, with α of the order of unity.

Although this model predicts that there are always two resonance modes, it is likely that only one, Ω_+, could be readily observed at magnetic fields used in the experiments, since Ω_- not only has very low frequency (~ 5 cm^{-1} for $\gamma=15$ cm^{-1} and $B=9$ T), which is out of the region of effective detection, but also is very weak ($\sim 10\%$ of the strength of the high-frequency mode at 9 T). Taking this into consideration, the single sharp line with position shifted to higher frequency at the lowest densities can be explained. At high field the linewidth Γ can be significantly smaller than the linewidth of CR at high densities determined from the transport scattering rate. Samples with lower mobility have larger impurity potential and number density, therefore larger pinning parameter γ, and larger transition frequency shift upward from ω_c. Reverse substrate bias increases γ, and hence broadens the line and shifts the peak position up. All of these qualitatively agree with the experimental results in the lowest filling factor region. However, a number of discrepancies exists between this model and experiment. First, the theory predicts that the linewidth should be inversely related to the magnetic field. This has not been observed in the experiments; there is no noticeable change in linewidth in the lowest ν region and with field ≤ 9 T (see Fig. 8); for one sample at 15 T, the linewidth is actually *larger* than that at lower field. In addition, the theory suggests that the frequency shift ($\Omega_+-\omega_c$) should have roughly the same magnitude as the linewidth Γ, independent of samples or fields. The experimental data show that the ratio of the frequency shifts between our lowest-mobility sample and the highest-mobility sample can be as large as 2.5–3, while the linewidth differences (in the lowest ν region) are less than 15%, clearly in disagreement with the theoretical prediction. Whether n_s or ν is the critical parameter to determine the line shape is not predicted clearly by this model since several parameters involved in the calculation are implicitly dependent on n_s and **B**. The multiple-line structure observed for intermediate values of ν certainly cannot be explained by this version of the charge-density wave (CDW) model proposed by Fukuyama and Lee.[9] More recently, some theoretical justification for the notion that the CDW may *vanish* at $\nu>1$ has been advanced.[24] If that is the case, the CDW theory offers no prediction for the behavior of the line shape in this filling factor region.

C. Magnetoplasmons and magnetic excitons

Low-density CR measurements have also been performed on GaAs/$Al_xGa_{1-x}As$ systems.[10–16] Schlesinger *et al.*[10] found an anomalous line broadening (or splitting for a lower mobility sample) and a frequency shift, very similar to the behavior observed on Si-MOS devices. To explain these anomalies, these authors proposed a model in which the cyclotron-resonance mode interacts with "softened" two-dimensional plasmon modes at finite wave vector **q**.

The dispersion relation of 2D magnetoplasmons, $\omega(q)$ relative to ω_c, has a minimum, which corresponds to a singularity in the density of states, at $ql_B\approx 2$, where $l_B=(ch/eB)^{1/2}$ is the magnetic length (see Fig. 12). The distance between the CR mode and the minimum of the plasmon dispersion curve was assumed to be an adjustable parameter, δ, so that the dispersion curve could be shifted arbitrarily. A model calculation showed an anti-level-crossing behavior in the absorption spectrum when δ changed from positive to negative values, which was used as a qualitative explanation for the experimental data. However, an answer to the question of why the 2D plasmon modes should be "softened" and move into resonance with the CR mode was not provided.

Kallin and Halperin[17] carried out a model calculation restricted to the case that the electron density and magnetic field are such that an integral number of Landau levels is exactly filled, and the magnetic field is sufficiently strong that the cyclotron energy is larger than the Coulomb energy. Under these restrictions, the screening effect can be neglected to lowest order, and there is no broadening in the excitation spectrum in the absence of

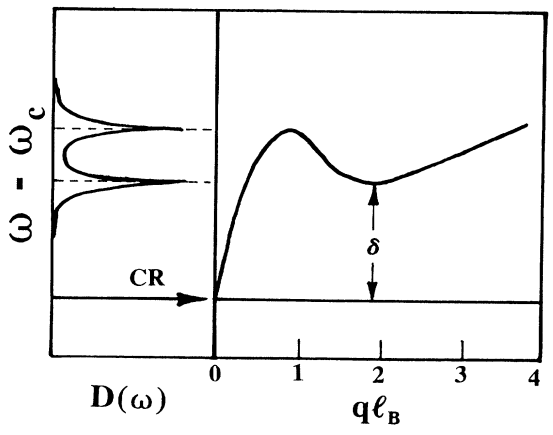

FIG. 12. Sketches of magnetoplasmon or magnetic exciton dispersion curve (right panel), and corresponding density of states (left panel). **q** is the wave vector of magnetoplasmon and l_B is the magnetic length (see text).

impurities. The elementary neutral excitations near ω_c may be described as magnetoplasmon modes, or magnetic excitons, in which one electron is excited to an unoccupied Landau level, leaving behind a hole in the filled Landau level. The exciton dispersion relation (schematically indicated in Fig. 12) and absorption spectrum can be calculated self-consistently. For filling factor $\nu=1$ and short-range impurity potentials corresponding to a reasonable sample mobility, the spectrum shows a double-line structure: a main peak shifted *downward* with extremely narrow linewidth and strong relative intensity, and a broad, very weak feature at $\omega>\omega_c$ due to the magnetoplasmon mode at the minimum of the dispersion curve (singularity in the density of states). As the mobility decreases, the relative intensity of the higher-frequency feature increases. It is possible for the higher-frequency line to dominate the spectrum; however, this will correspond to an extremely small mobility with respect to the mobilities of normal samples used in the experiments. Comparing with the magnetoplasmon model suggested by Schlesinger *et al.*,[10] the CR mode is indeed depressed due to the interaction with the high-lying magnetoplasmon (or magnetic exciton) modes. However, in order to observe an antilevel crossing and thus multiple (2) lines, the minimum of the exciton dispersion curve has to be lowered into the CR mode. This is possible only when higher-order corrections are considered, and it has been shown[25] that such corrections are too small to bring the minimum into resonance with CR mode.

An important result of this model calculation is the demonstration that the linewidth of an interacting system can be considerably smaller than that of a noninteracting system, in which the linewidth is determined by either the transport scattering rate or inhomogeneous broadening. However, the downward shift of the CR mode (depressed by the high-lying magnetoplasmon mode) seems to contradict the experimental observations, in which the resonance peak always has *higher* frequency than the unperturbed CR frequency (defined by the undressed band-edge effective mass) at the lowest filling factors (there is a general downward shift of the CR peak at filling factors *above* ν_c, which might be related to this prediction). However, the restriction of $\nu=1$ in this model makes direct comparison very difficult. Extensions of this model for $\nu<1$ have been carried out.[26] Screening for $\nu<1$ reduces the coupling between the CR mode and the magnetioplasmon (or magnetic exciton); hence it causes the CR mode to shift *upward* and narrows the linewidth simultaneously.[11] However, this upward shift due to the decoupling should never *exceed* the unperturbed CR frequency ω_c; thus it clearly cannot explain the present experimental results (or the results of Schlesinger *et al.* when the small nonparabolicity of GaAs is considered[4]). This model makes no prediction for the multiple-line structure in the crossover region of ν, nor any mobility-dependent behavior of the line shape, since it is intended for the weak localization situation.

Several other theoretical models and speculations have been advanced, e.g., electron-phonon coupling,[7] fractional quantum Hall effect,[15,16] filling-factor-dependent screening,[27] and impurity transitions in the presence of 2D magnetoplasmons.[28] Each is based on different physical considerations, and each can explain one or two experimental features. These models are either not closely related to the present phenomena, or are still too sketchy to make a detailed comparison with the present experiment useful. At present, no single model can adequately describe all of the observed anomalous features.

V. DISCUSSION AND CONCLUSIONS

Although the dependence of the center of gravity and the overall linewidth on filling factor appear similar to earlier work on Si,[7] the detailed results of the present experiments are quite different. Several important differences and crucial points should be emphasized. First, the anomalous behavior of the low-density "CR" is due to a multiple-line structure. The positions of the individual components are not dramatically changed, but their relative intensities vary strongly with filling factor. The previous measurements did not resolve multiple-line structures, apparently because of the higher-mobility (weaker localization) samples studied and poorer signal-to-noise ratio. Second, the filling factor dependence of the line shape is *not strict* as suggested by earlier work. The detailed line shape and critical filling factor depend on sample mobility. However, for a given sample, filling factor is indeed the parameter that correlates with line shape. Third, the magnitude of the anomalies increases systematically with decreasing mobility, i.e., poorer mobility samples have higher ν_c, clearer multiple-line structure, and larger frequency shift upward from the unperturbed CR position. This demonstrates that localization plays an important role. The results of substrate-bias-dependent measurements show that increasing the surface field, hence larger interface potential fluctuations, leads to larger shift upward in transition frequency in the lowest filling factor region, which indicates the importance of localization and is consistent with the results of mobility-dependent measurements. The present work has also shown that varying the surface crystallographic plane [vicinal to (001)] has little effect on the qualitative behavior of CR line shape.

The temperature-dependent measurements show that thermally populated localized electrons in the higher-lying fourfold valleys behave similarly to the electrons in the twofold valleys. This is consistent with the earlier work on Si-MOS devices[29] where uniaxial stress was used to tune the valleys into near coincidence and an upward shift of the transition frequency was observed for the fourfold valley at low n_s. In the present work for the transitions associated with the twofold valleys, raising temperature increases the linewidths, and the overall peak position shifts back to the unperturbed CR position in the crossover filling factor region. These results are in agreement with earlier work.[6,7,29] However, in the *lowest* filling factor region no significant position change was observed in the present work for either twofold or fourfold valleys at comparable temperatures, in contrast to Ref. 29 (fourfold valleys) and Refs. 6 and 7 (twofold valleys). It is likely that there are two sources underlying the

differences between this work and previous work:[7] (1) better signal-to-noise ratio in the present work, and (2) lower depletion charge combined with the fact that the temperature dependence measurements were carried out a lower electron densities (smaller splitting between twofold and fourfold valley, hence easier to populate fourfold valleys thermally) in the present case. These sources lead to a clear observation of distinguished double-line structure rather than an overall profile. The differences between the high and low filling factor results in the present work might be due to the differences between the magnitudes of the electron-electron correlations in the two cases. At lower filling factors the correlation energy is larger than that at higher filling factors (relative to Fermi energy); hence it is more difficult to destroy the correlated state thermally.

Random-potential fluctuations and localized states exist at the interfaces between two different materials for all types of semiconductor structures; thus it is useful to compare the present experimental results with the work on the GaAs heterostructure system to see what features are common to both systems. Richter *et al.*[30] have recently investigated the influence of impurity scatterers on CR in intentionally and selectively δ-doped $GaAs/Al_xGa_{1-x}As$ samples. The Be-acceptor doped (*repulsive* scatterers) heterostructures have mobilities of $\sim 22\,000$ $cm^2/V\,s$ (corresponding to ~ 7700 $cm^2/V\,s$ for Si when the effective-mass difference is taken into account), and a typical electron density of 2.6×10^{11} cm^{-2}, which corresponds to filling factor from 4.5 to 0.8 as magnetic field varies from 2.4 to 13.5 T in their experiment. A *double*-line structure was observed in a crossover filling factor region ($4>\nu>2$) with the high-frequency component increasing in absorption intensity at the expense of the low-frequency component as field was increased (ν decreased). At the lowest values of ν ($\nu<2$), only a single line appeared at frequency *above* the unperturbed CR position with the linewidth much narrower than that at large ν. The upward frequency shift monotonically increased as the acceptor concentration was increased (larger potential fluctuations). All of these behaviors are qualitatively very similar to the present results on Si-MOS samples. However, for samples with attractive scatterers (Si donors) very different behavior was found, namely the usual properties of a 2D free-electron gas in the presence of scattering centers, i.e., linewidth and transition frequency oscillate as a function of ν due to ν-dependent screening.[27] This drastic difference[30] clearly showed the importance of the dopant type, which has also been found in other work.[28,31] Here we give alternative considerations that we believe are important in explaining the salient features of *both* the GaAs and Si results, and thus provide a connection between these apparently disparate materials. Due to the large free-electron density in Ref. 30 (one order of magnitude larger than the dopant concentrations for either donors or acceptors), the acceptors are ionized (negatively charged) and the donors are neutralized in the usual single-particle picture. Coulomb repulsion between electron and ionized acceptor can generate long-range (compared to the cyclotron orbit size), randomly distributed potential fluctuations, and hence the localization potential for the electrons. In the case of neutralized donors, the interactions are short-range, and most of the excess electrons are not affected by these charge-neutral scattering centers; therefore they behave just like free electrons in the presence of short-range scatters. For the samples used in our experiments there is a random distribution of charge centers of both signs throughout the amorphous oxide, which leads to a large, long-range fluctuating potential that is "seen" by electrons in the Si. In addition, there is a short-range random potential due to surface roughness and interface states. Due to the lower electron densities at low filling factors relative to the density of localized states (presumably of range comparable to the cyclotron orbit size or larger), it is expected that localization will be very important. Other experimental work[10–16] on GaAs heterostructures studied samples with much higher mobilities (at least a factor of 5 larger than that of Ref. 30). A single line or much smaller splitting[10,14] were observed. All the above experiments point to potential fluctuations as the origin of the upward shift of the transition frequency in the quantum limit. Measurements of the temperature dependence of the CR linewidth in the quantum limit on the high-mobility $GaAs/Al_xGa_{1-x}As$ heterostructures[32] shows a single line with the linewidth continuously narrowing as temperature decreases, in qualitative agreement with our results for the twofold valleys.

A single-particle localization model has been used in Ref. 30 to interpret data on the sample with repulsive scatterers, and this simple model can also explain some of the features in the present work. However, it suffers several major shortcomings as pointed out in the preceding section. The *ad hoc* addition of filling-factor-dependent screening,[27,33] which as a maximum effect at half integral ν, and would reduce the frequency shift and linewidth at these values, cannot explain either the gradual monotonic decrease in the frequency shift and approximately constant linewidth below $\nu\simeq 1$ for all samples in our measurements, or the initial appearance of the narrowed line at different ν for different samples. In addition, CR linewidth oscillations, which were searched for at large filling factors as evidence of ν-dependent screening, were *not* observed within the experimental sensitivity and signal-to-noise ratio. This negative result argues against ν-dependent screening playing a significant role in this system and this phenomenon.

Electron-electron interaction is one of the dominant energies in this problem. The Coulomb repulsive energy between two electrons confined in the same potential well with ~ 200 Å diameter is approximately 6 meV, considerably larger than the typical magnitude of the fluctuating potential. Thus single electrons will tend to be localized in individual potentials, and details of the electron distribution in space will depend on the competition between the Coulomb repulsive energy and the magnitude of the potential fluctuations. To illustrate how Coulomb interaction affects the line shape, we consider a one-dimensional example with two electrons localized in harmonic-oscillator potentials separated by a distance D. The Hamiltonian can be written as

$$H = p_1^2/2m^* + \tfrac{1}{2}m^*\omega_1^2 x_1^2 + p_2^2/2m^* + \tfrac{1}{2}m^*\omega_2^2 x_2^2 + e^2/[\epsilon|D + (x_1 - x_2)|] ,$$

where x_1 and x_2 are coordinates of electrons relative to the potential centers, and ϵ is the dielectric constant. For strong localization ($D \gg x_1, x_2$), we may neglect the exchange interaction (no wave-function overlap) and treat the Coulomb term as a perturbation. To order $O[(x_1 - x_2)^2/D^2]$, the energy spectrum is

$$E = (N_1 + \tfrac{1}{2})\hbar\omega_1(1 + e^2/\epsilon D^3 m^* \omega_1^2) + (N_2 + \tfrac{1}{2})\hbar\omega_2(1 + e^2/\epsilon D^3 m^* \omega_2^2) + (e^2/\epsilon D)[1 + (e^2/\epsilon D^3 m^*)(\omega_1^{-2} + \omega_2^{-2})] .$$

The last term simply shifts the energy zero. The frequencies of electric-dipole-allowed transitions are $\hbar\omega_1(1 + e^2/\epsilon D^3 m^* \omega_1^2)$ and $\hbar\omega_2(1 + e^2/\epsilon D^3 m^* \omega_2^2)$, respectively. Physically the Coulomb repulsion increases the confinement and thus the transition energies, with the largest upward shift occurring for the weakest potential. Of course, a real physical system is much more complicated than this example, but the basic physics should be qualitatively similar. The Coulomb interaction among the electrons shifts the transition frequencies of all localized single electrons upward and *narrows* any inhomogeneously broadened line profile,[34] in qualitative agreement with the experimental observations at the lowest filling factors. Although this simple perturbation method is clearly not appropriate for quantitative estimates, since electron-electron interaction is the same order of magnitude as the confining potential, it is nevertheless generally true that the linewidth narrows when the interaction is introduced because of the correlation in the electron motion.[17]

The multiple-line structure and the variation of the relative intensity of each component with filling factor are not predicted either by the single-particle localization model or by existing many-body calculations. We suggest that spin-valley splitting of the Landau levels coupled with electron correlations is a possible explanation. The electron-exchange interaction greatly enhances the spin-valley splitting and couples the spin and valley states.[35,36] The magnitude of the exchange energy depends on Landau-level occupancy (filling factor ν), and is largest for the lowest Landau level. Coupled states with the energy separation dependent on ν could have different transition selection rules than the normal situation (i.e., interspin and intervalley transitions become dipole allowed), which could lead to a multiple-line structure for $\nu < 4$. The discrepancy between the number of components observed in the present experiments and those of Ref. 30 is understandable in this context since there is no valley degeneracy in GaAs. However, the dependence on mobility is not obvious; there are no calculations for the exchange effects for electrons localized in random potentials in high magnetic fields to the best of our knowledge. It is apparent that both localization and many-body interaction are required in order to understand the anomalies in low-density cyclotron resonance; the relative importance depends on the quality of the structures investigated.

Finally, we summarize our conclusions briefly as follows. The CR line-shape anomalies at low filling factors originate from the multiple-line structure and relative intensity variations among the components as a function of filling factor. The amplitude of anomalies exhibits a systematic sample mobility dependence, which demonstrates the importance of localization. Several experimental results are qualitatively consistent with single-particle localization models; however, the filling factor dependence, the dramatically narrowed linewidth as $\nu \to 0$, and the number of observed lines cannot be explained by these models. The *ad hoc* inclusion of the simple form of ν-dependent screening is also not capable of explaining the CR anomalies in this system. The electron-electron interaction distributes electrons in such a way as to form a short-range order to minimize the total energy, and it tends to narrow the inhomogeneously broadened CR line in comparison with the single-particle model. Spin-valley splitting enhanced by the exchange interaction in the lowest Landau levels provides a possible explanation for the multiple-line structure; however, detailed calculations of this effect on the CR of localized electrons are needed to clarify this speculation. We expect a complete theory should include both localization and many-body effects on an equal footing.

ACKNOWLEDGMENTS

We thank N. C. Jarosik for the initial measurements, Y. C. Lee for many stimulating discussions, and J.-M. Mercy, Y.-H. Chang, E. R. Glaser, G. Brozak, A. A. Reeder, and W. J. Li for assistance in various aspects of the experiments. High-magnetic-field measurements were carried out at the Francis Bitter National Magnet Laboratory; we are indebted to the staff, especially B. Brandt, for their help. This work was supported in part by the Office of Naval Research under Grant No. N0001489-J-1673.

[1]T. Ando, A. B. Fowler, and F. Stern, Rev. Mod. Phys. **54**, 437 (1982).

[2]K. von Klitzing, G. Dorda, and M. Pepper, Phys. Rev. Lett. **45**, 494 (1980).

[3]D. Tsui, H. L. Störmer, and A. C. Gossard, Phys. Rev. Lett. **50**, 1953 (1983).

[4]For a brief review, see A. Petrou and B. D. McCombe, in *Landau Level Spectroscopy*, edited by G. Landwehr and E. I. Rashba, Modern Problems in Condensed Matter Sciences (North-Holland, Amsterdam, 1991), Vol. 27

[5]G. Abstreiter, J. P. Kotthaus, J. F. Koch, and G. Dorda, Phys. Rev. B **14**, 2480 (1976).

[6]R. J. Wagner, T. A. Kennedy, B. D. McCombe, and D. C. Tsui, Phys. Rev. B **22**, 945 (1980).
[7]B. A. Wilson, S. J. Allen, and D. C. Tsui, Phys. Rev. Lett. **44**, 479 (1980); Phys. Rev. B **24**, 5887 (1981).
[8]H.-J. Mikeska and H. Schmidt, Z. Phys. B **20**, 43 (1975).
[9]H. Fukuyama and P. A. Lee, Phys. Rev. B **18**, 6245 (1978).
[10]Z. Schlesinger, S. J. Allen, J. C. M. Hwang, P. M. Platzman, and N. Tzoar, Phys. Rev. B **30**, 435 (1984).
[11]Z. Schlesinger, W. I. Wang, and A. H. MacDonald, Phys. Rev. Lett. **58**, 73 (1987).
[12]K. Ensslin, D. Heitman, H. Sigg, and K. Ploog, Phys. Rev. B **36**, 8177 (1987).
[13]M. J. Chou, D. C. Tsui, and G. Weimann, Phys. Rev. B **37**, 848 (1988).
[14]E. Batke, H. L. Störmer, A. C. Gossard, and J. H. English, Phys. Rev. B **37**, 3093 (1988).
[15]G. L. J. A. Rikken, H. W. Myron, P. Wyder, G. Weimann, W. Schlapp, R. E. Horstman, and J. Wolter, J. Phys. C **18**, L137 (1985).
[16]W. Seidenbusch, E. Gornik, and G. Weimann, Phys. Rev. B **36**, 9155 (1987).
[17]C. Kallin and B. I. Halperin, Phys. Rev. B **31**, 3635 (1985).
[18]J.-P. Cheng and B. D. McCombe, Phys. Rev. Lett. **64**, 3177 (1990).
[19]P. Richman, *MOS Field-Effect Transistor and Integrated Circuits* (Wiley, New York, 1973).
[20]L. E. DeLong, O. G. Symko, and J. C. Wheatley, Rev. Sci. Instrum. **42**, 147 (1971); N. C. Jarosik, Ph.D. thesis, State University of New York at Buffalo, 1985.
[21]J.-P. Cheng and B. D. McCombe, Phys. Rev. B **38**, 10 974 (1988).
[22]E. Glaser and B. D. McCombe, Phys. Rev. B **37**, 10 769 (1988).
[23]E. Wigner, Phys. Rev. **46**, 1002 (1934).
[24]D. Yoshioka and H. Fukuyama, J. Phys. Soc. Jpn. **47**, 394 (1979).
[25]A. H. MacDonald, J. Phys. C **18**, 1003 (1985).
[26]A. H. MacDonald, H. C. A. Oji, and S. M. Girvin, Phys. Rev. Lett. **55**, 2208 (1985).
[27]R. Lassnig and E. Gornik, Solid State Commun. **47**, 959 (1983).
[28]S. R. E. Yang and A. H. MacDonald, Phys. Rev. B **42**, 10 811 (1990).
[29]P. Stallhofer, J. P. Kotthaus, and G. Abstreiter, Solid State Commun. **32**, 655 (1977).
[30]J. Richter, H. Sigg, K. v. Klitzing, and K. Ploog, Phys. Rev. B **39**, 6268 (1989).
[31]R. J. Haug, R. R. Gerhardts, K. von Klitzing, and K. Ploog, Phys. Rev. Lett. **59**, 1349 (1987).
[32]C. T. Liu, P. Mensz, D. C. Tsui, and G. Weimann, Phys. Rev. B **40**, 1716 (1989).
[33]D. Heitmann, M. Ziesmann, and L. L. Chang, Phys. Rev. B **34**, 7463 (1986).
[34]Kohn's theorem, which states that the electron-electron interaction does not affect the CR in a homogeneous system with a translational invariance [W. Kohn, Phys. Rev. **123**, 1242 (1961)], is not applicable here, since the random-potentail fluctuations break the translational symmetry.
[35]W. L. Bloss, L. J. Sham, and B. Vinter, Phys. Rev. Lett. **43**, 1529 (1979).
[36]G. F. Giuliani and J. J. Quinn, Phys. Rev. B **31**, 6228 (1985).